IOPscience iopscience.iop.org

Home Search Collections Journals About Contact us My IOPscience

Linear response theory of inter-quantum-well tunnelling in a double-well structure with in-plane magnetic fields

This article has been downloaded from IOPscience. Please scroll down to see the full text article.

1993 J. Phys.: Condens. Matter 5 L299

(http://iopscience.iop.org/0953-8984/5/22/001)

View the table of contents for this issue, or go to the journal homepage for more

Download details:
IP Address: 171.66.16.96
The article was downloaded on 11/05/2010 at 01:20

Please note that terms and conditions apply.

J. Phys.: Condens. Matter 5 (1993) L299–L306. Printed in the UK

LETTER TO THE EDITOR

Linear response theory of inter-quantum-well tunnelling in a double-well structure with in-plane magnetic fields

S K Lyo and J A Simmons
Sandia National Laboratories, Albuquerque, NM 87185, USA

Received 9 March 1993

Abstract. A linear response theory of incoherent tunnelling is presented and compared to data for the 2D–2D inter-quantum-well conductance for a double-well structure with an external in-plane magnetic field. The tunnelling conductance, calculated by evaluating the current–current correlation function, shows resonances as a function of the magnetic field. The widths and heights of the resonance peaks depend sensitively on the intra-well scattering times and temperature. Tunnelling occurs not only through the ground-energy sublevels but also through the higher-energy sublevels which can be important at high temperatures. Using a differential transmission-line model, analytic relationships between the source–drain conductance and the tunnelling conductance are derived. The theoretical results yield reasonable agreement with the tunnelling conductance data obtained from this relationship.

Tunnelling between two adjacent quasi-two-dimensional quantum wells (QWs) has received increasing attention recently not only for its academic interest but also for a potential device application. In spite of basic intuitive understanding [2] of existing experimental results [1, 2], a rigorous theoretical treatment and a quantitative comparison of the theoretical result with the data are still lacking. The purpose of this paper is threefold. First, we establish a rigorous theory of tunnelling conductivity. Second, we develop a general theory for the relationship between the source–drain resistance and tunnelling conductance. We apply the result to two structures, one studied recently by Eisenstein, Gramila, Pfeiffer and West (EGPW) [2] and the other to be discussed here. Finally, we compare our theory to tunnelling conductance data of our structure obtained from the measured source–drain conductance through this relationship. Experimentally, two 150 Å wide GaAs QWs are separated by a 65 Å $Al_{0.3}Ga_{0.7}As$ barrier. A 250 Å wide 10^{18} cm^{-3} Si-doped region is 450 Å above the top well, while a 7×10^{11} cm^{-2} Si delta-doped layer lies 800 Å beneath the bottom well. Tunnelling is controlled locally on a micron scale by using gates in our structure.

In our linear response theory, the tunnelling conductance is calculated by evaluating the current–current correlation function. Electrons drift into the first QW (QW1), tunnel through the barrier into the second QW (QW2) and then flow out of the second QW under the influence of a linear external DC electric field. The two QWs under study have two-dimensional electron densities N_1, N_2 with Fermi energies ϵ_{1F}, ϵ_{2F} and Fermi wave numbers k_{1F} and k_{2F}, respectively. We consider widely separated QWs; the tunnelling integral J_κ is much smaller than the damping (Γ_κ) of the level so that electrons undergo many intra-well scattering events before tunnelling into the other well. Here κ denotes a state label.

0953-8984/93/220299+08$07.50 © 1993 IOP Publishing Ltd

Before introducing our theory, we give a brief description of the underlying basic physics behind 2D–2D tunnelling. The energy and momentum conservation conditions cannot be satisfied simultaneously in the case $N_1 \neq N_2$, because the Fermi surfaces (i.e. circles) of QW1 and QW2 have different radii (i.e. $k_{1F} \neq k_{2F}$) and do not overlap. However, in the presence of an external in-plane magnetic field B (in the x-direction), the centre of the Fermi circle of QW2 shifts in the $k = (k_x, k_y)$ plane by an amount $\Delta k_y \propto B$ relative to that of QW1 [2, 3]. As the field increases from $B = 0$, the two Fermi circles begin to touch each other from the inside of the larger circle at $B = B_-$. Upon increasing the field further, the two Fermi circles cross each other until the field reaches B_+ and the two Fermi circles begin to separate [2]. Resonant tunnelling is possible only for fields in the range $B_- \leqslant B \leqslant B_+$. The tunnelling current, however, is not readily calculable by the golden rule, because, as will be shown later, the final result depends on the total scattering rates out of the resonance states in both QWs. Therefore, it is necessary to develop a formal theory that can properly incorporate the effect of scattering inside the QWs. Intra-well scattering of the electrons is due to elastic and inelastic collisions. We find that the tunnelling rate (as well as the 2D–2D conductance) depends sensitively on the intra-well scattering times. In our theory, tunnelling occurs not only through the ground-energy sublevels but also through the higher-energy sublevels which can be important at high temperatures because of their larger tunnelling integrals.

Before studying the double-QW structure, we first consider the effect of applying an in-plane magnetic field (in the x-direction) on the electronic energy in a single isolated QW. In this case, the Hamiltonian is given (in an effective-mass approximation) by

$$H = (\hbar k_x)^2/2m_x^* + (\hbar^2/2m_y^*)(k_y - z/l^2)^2 + p_z^2/2m_z^* + V(z) \qquad (1)$$

where $l = \sqrt{\hbar c/eB}$ is the magnetic length, e is the electronic charge and m_i^* $(i = x, y, z)$ is the effective mass in the i-direction. The quantities $\hbar$ and c denote Planck's constant divided by 2π and the speed of light, respectively. The crystal momentum k is a good quantum number. In (1), $V(z)$ is the confinement potential energy and p_z is the momentum operator.

The eigenvalues of the Hamiltonian in (1) were studied earlier by Lyo and Jones (LJ) [4] and we review some of its properties briefly in the following. In order to provide some insight for the solution of (1), it is useful to consider the special case of a parabolic QW with $V(z) = \frac{1}{2}m_z^*\omega_0^2(z - z_0)^2$, where m_z^* and ω_0 are constants with units of mass and angular frequency and z_0 is the centre of the potential. In this case, the net effect of the magnetic field on the energy eigenvalue is to renormalize ω_0 into $\Omega = \lambda\omega_0$ and m_y^* into $M_y^* = \lambda^2 m_y^*$ where $\lambda^2 = 1 + (m_y/m_z)(\omega_c/\omega_0)^2$ and ω_c is the cyclotron frequency $\omega_c = eB/m_y^*c$ [4]. Also, z is replaced by z_0 in the second term of (1). The second term in λ^2 reflects mixing between the sublevels and the field-induced z-dependent terms and is proportional to the square of the ratio of the representative energies, namely the cyclotron energy and the field-free sublevel energy separation ($\hbar\omega_0$). The magnetic field pushes the centroid of the harmonic confinement wavefunction toward the interface of the QW [4]. It was found by LJ that the enhancement factor λ is very close to unity and the field-induced shift of the centroid of the wavefunction is negligibly small, unless the field is extremely high and the QW is very wide and shallow [4]. A very similar conclusion was drawn for square QWs to be considered here [4]; the energy dispersion in the y-direction is nearly parabolic with very small mass enhancement in the range of the field and for the QW structure of interest in this work. Also, field-induced mixing between k_y and the sublevels is small.

In the following analysis, we assume an isotropic in-plane mass m^*. We also assume that both QWs have the same effective mass. A tight-binding model is adequate for studying

incoherent tunnelling between two widely separated QWs. The Hamiltonian of a double-QW structure is then given from the preceding analysis by

$$\mathcal{H} = \sum_{\kappa} (\epsilon_{1\kappa} a_{1\kappa}^{\dagger} a_{1\kappa} + \epsilon_{2\kappa} a_{2\kappa}^{\dagger} a_{2\kappa} + J_{\kappa}(a_{1\kappa}^{\dagger} a_{2\kappa} + a_{2\kappa}^{\dagger} a_{1\kappa})) + \mathcal{H}_{\text{int}} \tag{2}$$

where $\kappa = (k, \nu)$, ν is the sublevel index and $a_{n\kappa}^{\dagger}(a_{n\kappa})$ indicates the creation (annihilation) operator in the nth QW. The dependence of the tunnelling integral J_{κ} on k and the magnetic field will be neglected in view of the discussion in the previous paragraph. The electron energy is given by

$$\begin{aligned} \epsilon_{1\kappa} &= (\hbar k)^2/2m^* + \Delta_{1\nu} \\ \epsilon_{2\kappa} &= (\hbar k_x)^2/2m^* + \hbar^2(k_y - \Delta k_y)^2/2m^* + \Delta_{2\nu} \end{aligned} \tag{3}$$

where $k = |k|$, $\Delta k_y = d/l^2$ and d is the centre-to-centre distance between the QWs. The quantity $\Delta_{n\nu}$ indicates the relative energies of the sublevels and is determined from N_1 and N_2. Finally, the last term in (2) describes elastic and inelastic interactions responsible for intra-QW scattering.

The tunnelling conductivity is given from the linear response theory [5] by

$$\sigma_{zz} = \frac{e^2}{i\Omega} \lim_{\omega \to 0} \frac{\mathcal{F}(\hbar\omega + i0) - \mathcal{F}(i0)}{\omega} \tag{4}$$

where $\Omega = Sd$ (S is the effective tunnelling area of the QW),

$$\mathcal{F}(\omega_r) = \int_0^{\beta} F(u) \exp(\hbar\omega_r u)\, du \tag{5}$$

$$\begin{aligned} F(u) &= \langle \hat{v}_z(u) \hat{v}_z(0) \rangle \\ \hat{v}_z(u) &= \exp(u\mathcal{H}) \hat{v}_z \exp(-u\mathcal{H}) \end{aligned} \tag{6}$$

and $\beta = (k_B T)^{-1}$. Here k_B is Boltzmann's constant and T the temperature. The quantity $\hbar\omega_r$ is defined on the imaginary axis as $\hbar\omega_r = 2\pi i r \beta^{-1}$ and is analytically continued to just above the real axis: $\hbar\omega + i0$ or $i0$ as in (4). The velocity operator in (6) is given by

$$\hat{v}_z = [\hat{z}, \mathcal{H}]/i\hbar = (J_{\kappa} d/i\hbar)(a_{1\kappa}^{\dagger} a_{2\kappa} - a_{2\kappa}^{\dagger} a_{1\kappa}). \tag{7}$$

Here $\hat{z}$ is the position operator given by $\hat{z} = z_1 a_{1\kappa}^{\dagger} a_{1\kappa} + z_2 a_{2\kappa}^{\dagger} a_{2\kappa}$, where z_1 and $z_2 (= z_1 + d)$ are the positions of the centre of the two QWs assumed to be symmetric.

The conductivity σ_{zz} is evaluated using a temperature-ordered Green function technique [6]; the main contribution to the velocity correlation function $\mathcal{F}(\hbar\omega_r)$ is given, to the lowest order in $\Gamma_{n\text{F}}/\epsilon_{n\text{F}}$, by the bubble diagram shown in figure 1. Here $\Gamma_{n\text{F}}$ is the damping at the Fermi circles. The vertex correction is small when $\epsilon_{1\text{F}} - \epsilon_{2\text{F}} \gg \Gamma_{n\text{F}}$ as in our case. In figure 1, the wiggly directed lines indicate the external-field vertices signifying the tunnelling velocity $v_z = J_{\kappa} d/\hbar$ and the full curves represent dressed fermion propagators in QW1 (directed downward) and QW2 (directed upward) given by

$$G_{n\kappa}(\zeta_l) = [\zeta_l - \epsilon_{n\kappa} - S_{n\kappa}(\zeta_l)]^{-1} \qquad n = 1, 2 \tag{8}$$

where $\zeta_l = (2l+1)\pi i\beta^{-1} + \mu$, l is an integer, μ the chemical potential and $S_{n\kappa}(\zeta_l)$ is the self-energy part. The self-energy arises from the last term in (2). The velocity correlation function $\mathcal{F}(\hbar\omega_r)$ is then given by

$$\mathcal{F}(\hbar\omega_r) = -(4d^2/\beta\hbar^2)\sum_{l\kappa} J_\kappa^2 G_{1\kappa}(\zeta_l)G_{2\kappa}(\zeta_l + \hbar\omega_r) \tag{9}$$

which includes a factor of two arising from the spin degeneracy and a minus sign arising from closing the fermion loop. The spin splitting is neglected. The l-summation in (9) is performed on a complex plane [6]. Inserting (9) in (4), we obtain

$$\sigma_{zz} = \frac{4\pi e^2 d^2}{\Omega\hbar}\sum_\kappa J_\kappa^2 \int_{-\infty}^{\infty} [-f'(\zeta)]\rho_{1\kappa}(\zeta)\rho_{2\kappa}(\zeta)\,d\zeta \tag{10}$$

where

$$\rho_{n\kappa}(\zeta) = \frac{1}{\pi}\operatorname{Im} G_{n\kappa}(\zeta - i0) = \frac{1}{\pi}\frac{\Gamma_{n\kappa}(\zeta)}{(\zeta - \epsilon_{n\kappa} - \sum_{n\kappa}(\zeta))^2 + \Gamma_{n\kappa}(\zeta)^2} \qquad n = 1, 2 \tag{11a}$$

and $f'(\zeta)$ is the first derivative of the Fermi function $f(\zeta)$, Im denotes the imaginary part of the quantity that follows and $S_{n\kappa}(\zeta - i0) = \Sigma_{n\kappa}(\zeta) + i\Gamma_{n\kappa}(\zeta)$. For a later numerical evaluation, we approximate

$$\rho_{n\kappa} \simeq (1/\pi)\Gamma_{nF}/[(\zeta - \epsilon_{n\kappa})^2 + \Gamma_{nF}^2] \qquad n = 1, 2 \tag{11b}$$

at low temperatures neglecting the small quasi-particle renormalization (i.e. the real part of the self-energy) and assuming that only the ground sublevels are populated. In the present work, application is made to the data at 0.3 K $\ll \epsilon_{nF}k_B^{-1}$, where tunnelling occurs mainly through the ground-energy sublevels. The damping $\Gamma_{n\kappa}(\zeta)$ has been studied by a number of authors in the past in QWs for elastic scattering, electron–phonon scattering and also for electron–electron scattering [7]. At low temperatures, the only major contribution to the damping arises from elastic scattering.

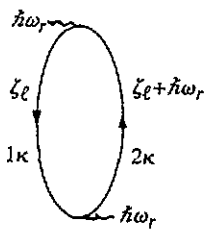

Figure 1. Basic bubble diagram for the velocity correlation function. The arrows indicate the flow of momentum (k) and energy parameters ($\zeta_l, \hbar\omega_r$).

In order to relate σ_{zz} to the source–drain resistance, we consider a differential transmission-line model for the two structures illustrated in figure 2, where the top full line indicates QW2 and the bottom full line QW1. In structure (a), the current enters QW1 and QW2 at $x = 0$ and flows out of both QWs at the other end. The gate (denoted by a shaded square) on the top QW is biased and blocks the current in the top QW. The wiggly

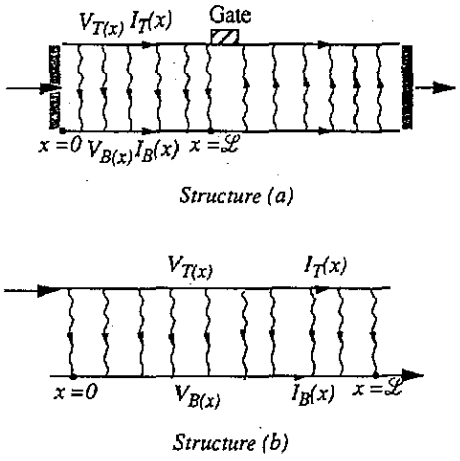

Figure 2. Transmission-line model for two tunnelling structures considered.

lines indicate the tunnelling current. In structure (b) studied recently by EGPW [2], the current drifts into the left-hand end of QW2 and flows out of the right-hand end of QW1. The source–drain resistance in structure (a) consists of the sum of three contributions: $R_{SD} = R_{SG} + R_G + R_{GD}$. Here R_{SG} is the resistance from the source (at $x = 0$) to the left-hand end of the gate (at $x = \mathcal{L}$), R_G is the contribution from the region under the gate in the bottom QW only and R_{GD} is the contribution from the right-hand end of the gate to the drain. We will consider only R_{SG} in the following. The tunnelling resistance in the S–G region is given by $R_{zz} = d/(S_{SG}\,\sigma_{zz})$, where S_{SG} is the area in the S–G region. For structure (b), we calculate the total resistance from the source (at $x = 0$) to the drain (at $x = \mathcal{L}$). In this case, the tunnelling resistance is given by $R_{zz} = d/(S\sigma_{zz})$.

Designating the current as $I_T(x)(I_B(x))$ and the voltage as $V_T(x)(V_B(x))$ for the top (bottom) wire and using the current conservation $I = I_T(x) + I_B(x)$, we obtain the following coupled differential equations:

$$I_\alpha(x) = -(1/\mathcal{R}_\alpha)\mathrm{d}V_\alpha(x)/\mathrm{d}x \qquad \alpha = \mathrm{T}, \mathrm{B} \tag{12a}$$

$$\mathrm{d}I_T(x)/\mathrm{d}x = -\mathrm{d}I_B(x)/\mathrm{d}x = -(1/\mathcal{R}_{zz}\mathcal{L}^2)(V_T(x) - V_B(x)) \tag{12b}$$

where $\mathcal{R}_T$ ($\mathcal{R}_B$) is the resistance per unit length in the top (bottom) wire, $\mathcal{L}$ is the total effective length of the wires and $\mathcal{R}_{zz} = R_{zz}/\mathcal{L}$. A general solution of these equations is given by

$$V_\alpha(x) = [\mathcal{R}_\alpha s_\alpha/(\mathcal{R}_T + \mathcal{R}_B)](c_1 \cosh(qx) + c_2 \sinh(qx)) + c_3 x \qquad \alpha = \mathrm{T}, \mathrm{B} \tag{13}$$

where $s_T = 1$, $s_B = -1$, $q = \mathcal{L}^{-1}[\mathcal{R}_T + \mathcal{R}_B)/\mathcal{R}_{zz}]^{1/2}$ and c_is are constants to be determined by the boundary conditions.

The boundary conditions are given by $V_T(0) = V_B(0) = 0$, $I_T(\mathcal{L}) = 0$ for structure (a) and $I_B(0) = 0$, $I_T(\mathcal{L}) = 0$ for structure (b). Also, the current conservation condition applies to both structures. The resistances are then given by

$$R_{SG} = \frac{\mathcal{R}_B^2 \mathcal{L}}{\mathcal{R}_T + \mathcal{R}_B}\frac{\tanh(q\mathcal{L})}{q\mathcal{L}} + \frac{\mathcal{R}_T \mathcal{R}_B \mathcal{L}}{\mathcal{R}_T + \mathcal{R}_B} \qquad \text{structure (a)} \tag{14a}$$

$$R_{SD} = \frac{\mathcal{R}_T \mathcal{R}_B \mathcal{L}}{q\mathcal{L}(\mathcal{R}_T + \mathcal{R}_B)}\left(\frac{2}{\sinh(q\mathcal{L})} + \frac{\mathcal{R}_T^2 + \mathcal{R}_B^2}{\mathcal{R}_T \mathcal{R}_B}\coth(q\mathcal{L}) + q\mathcal{L}\right) \qquad \text{structure (b).} \tag{14b}$$

Equations (14*a*) and (14*b*) yield $R_{SG} = \mathcal{L}\mathcal{R}_B$, and $R_{SD} = R_{zz}$, respectively, in the limit $q\mathcal{L} \ll 1$ (i.e. $\mathcal{R}_T + \mathcal{R}_B \ll \mathcal{R}_{zz}$) as expected. The QWs studied by EGPW [2] have high mobilities and yield $R_{SD} \simeq R_{zz}$. The tunnelling resistance R_{zz} enters (14*a*) and (14*b*) only through the factor q. For structure (a), the total source–drain resistance R_{SD} is the sum of R_{SG}, R_G and R_{GD}. The latter is obtained in a similar way from (14*a*). The quantity R_G is small.

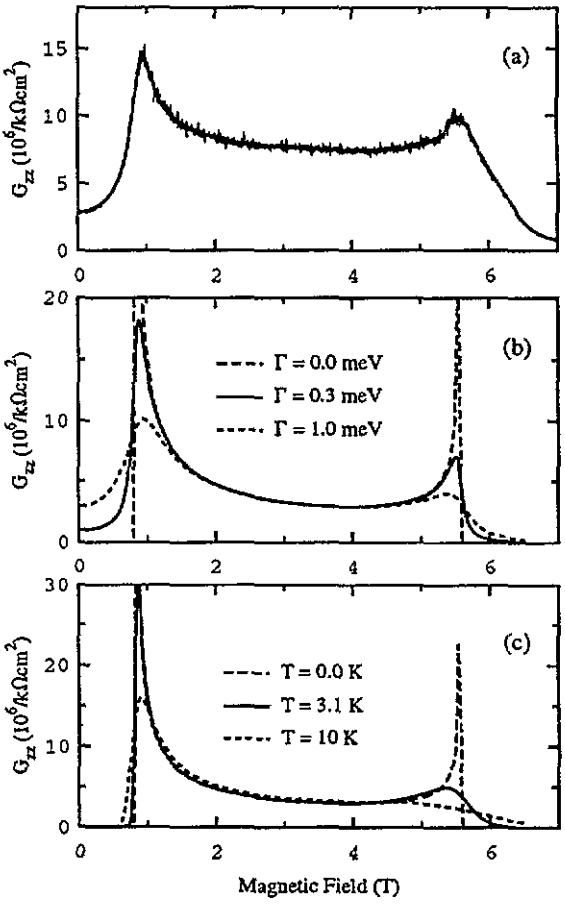

Figure 3. The tunnelling conductance per area $G_{zz} \equiv \sigma_{zz}/d$ determined from the observed source–drain resistance (*a*) and theory (*b*). The tunnelling conductance per unit area is also plotted for zero damping at several temperatures (*c*).

In figure 3(*a*), we plot the total tunnelling conductance per area of the QW ($G_{zz} \equiv \sigma_{zz}/d$) determined from the observed values of R_{SD} at 0.3 K using (14*a*). A detailed description of the experiment will be presented elsewhere [8]. The resistances of the top and bottom QWs equal 0.77 kΩ and 4.93 kΩ for these data, respectively. For comparison with the theory, the following experimentally determined parameters are used. The area and the centre-to-centre separation of the QWs are $S = 15\ \mu\text{m} \times 2\ \mu\text{m} = 3 \times 10^{-7}$ cm^2 and $d = 215$ Å. The densities and the mobilities of the bottom and top QWs are $N_1 = 1.74 \times 10^{11}$ cm^{-2}, $N_2 = 0.95 \times 10^{11}$ cm^{-2} and $\mu_1 = 6 \times 10^4$ cm^2 V^{-1} s^{-1}, $\mu_2 = 6 \times 10^5$ cm^2 V^{-1} s^{-1},

respectively. It follows that Γ_1 is about ten times larger than Γ_2. In this case (i.e. $\Gamma_2 \ll \Gamma_1$), we can simplify the expression in (10) using $\rho_{2\kappa} \simeq \delta(\zeta - \epsilon_{2\kappa})$ for (11*b*), where $\delta(x)$ is the Dirac delta function. As a result, the tunnelling conductance becomes independent of Γ_2.

The theoretical tunnelling conductance per area is displayed as a function of the magnetic field in figure 3(*b*) for $\Gamma_1 = 0$ meV, $\Gamma_1 = 0.3$ meV and $\Gamma_1 = 1.0$ meV, using $m^* = 0.067m_0$ (m_0 is the free electron mass) and $J_1 = 0.04$ meV. This value of the tunnelling integral is in the neighbourhood of $J_1 = 0.03$ meV estimated by calculating the energy repulsion between the ground sublevels of the two QWs from our double-well structure. The minimum of Γ_1 for the mobility $\mu_1 = 6 \times 10^4$ cm^2 V^{-1} s^{-1} equals 0.15 meV for isotropic scattering and corresponds to the scattering time $\tau = 2.3 \times 10^{-12}$ s. It is seen in figure 3(*b*) that both of the sharp peaks at $\Gamma_1 = 0$ are smeared out by the damping effect. These peaks have long Lorentzian tails and are different from what is expected from thermal broadening. In figure 3(*c*), we plot the theoretical conductance per area as a function of the magnetic field at several temperatures for zero damping (i.e. $\Gamma_1 = \Gamma_2 = 0$) using the same values for the rest of the parameters as in figure 3(*b*); thermal broadening yields a very (i.e. exponentially) short tail for the low-field peak at temperatures comparable to the energies of the damping parameters employed for figure 3(*b*).

For the special case of zero damping and zero temperature, the field dependence of σ_{zz} is simply given from (10) by $\sigma_{zz} = C(1-u)^{-1/2}B^{-1}$ for $u < 1$ and $\sigma_{zz} = 0$ for $u > 1$, where

$$u = [dl^{-2} + d^{-1}l^2(k_{1F}^2 - k_{2F}^2)]^2/(8\pi N_1)$$

and

$$C = em^{*2}cJ^2/(\pi\hbar^4).$$

Here J is the tunnelling integral between the ground sublevels. The conductance per unit area is shown in this case by the long-dashed curves in figures 3(*b*) and 3(*c*) and is non-vanishing only in the range of the fields $B_- \leqslant B \leqslant B_+$. The turn-on ($B_-$) and turn-off ($B_+$) fields are given by the solutions of $u = 1$:

$$B_\pm = \hbar c\sqrt{2\pi}(\sqrt{N_>} \pm \sqrt{N_<})/ed = 16.505(\sqrt{N_>} \pm \sqrt{N_<})d^{-1}$$

where $N_>$ ($N_<$) is the larger (smaller) of N_1 and N_2. For the last equality, N_1 and N_2 are in units of 10^{12} cm^{-2} and B and d are, respectively, in units of Tesla and 100 Å. The densities N_1 and N_2 can therefore be determined from the turn-on and turn-off fields.

In summary, we presented a linear response theory of 2D–2D incoherent tunnelling and compared to tunnelling conductance data in a double-quantum-well structure in the presence of external in-plane magnetic fields. The tunnelling conductivity was calculated by evaluating the current–current correlation function. The conductance exhibits resonances as a function of the magnetic field. The widths and the heights of the resonance peaks depend sensitively on the intra-well scattering times and the temperature. The theory incorporates tunnelling not only through the ground-energy sublevels but also through the higher-energy sublevels which can be important at high temperatures. Using a differential transmission-line model, a useful analytic relationship between the source–drain conductance and the tunnelling conductance was derived. Tunnelling conductance data were obtained from the observed source–drain resistance as a function of the magnetic field using this relationship. The conductance data yield reasonable agreement with the theoretical results.

This work was supported by the Division of Materials Science, Office of Basic Energy Science, US DOE under Contract No DE-AC04-76DP00789.

References

[1] Smoliner J, Demmerle W, Berthold G, Gornick E, Weiman G and Schlapp W 1990 *Phys. Rev. Lett.* **63** 1374
[2] Eisenstein J P, Gramila T J, Pfeiffer L N and West K W 1991 *Phys. Rev.* B **44** 6511
[3] Hayden R K, Maude D K, Eaves L, Valadares E C, Henini M, Sheard F W, Hughes O H, Portal J C and Curry L 1991 *Phys. Rev. Lett.* **66** 1749
[4] Lyo S K and Jones E D 1992 *Solid State Commun.* **83** 975
[5] Holstein T and Friedman L 1968 *Phys. Rev.* **165** 1019
[6] Holstein T 1964 *Ann. Phys., NY* **29** 410
[7] Lyo S K 1991 *Phys. Rev.* B **43** 7091
[8] Simmons J A, Lyo S K, Klem J F, Sherwin M E and Wendt J R 1993 *Phys. Rev.* B **47** at press